Electronic Supplementary Material (ESI) for CrystEngComm.

Supporting information

Luminescence sensing and supercapacitor performances of a new (3, 3)-connected Cd-MOF

Qian-Qian Liu, Ke-Fen Yue*, Xian-Jun Weng and Yao-Yu Wang

Key Laboratory of Synthetic and Natural Functional Molecule Chemistry of the Ministry of Education, National Demonstration Center for Experimental Chemistry Education, College of Chemistry and Materials Science, Northwest University, Xi'an 710069, PR China

E-mail address: ykflyy@nwu.edu.cn

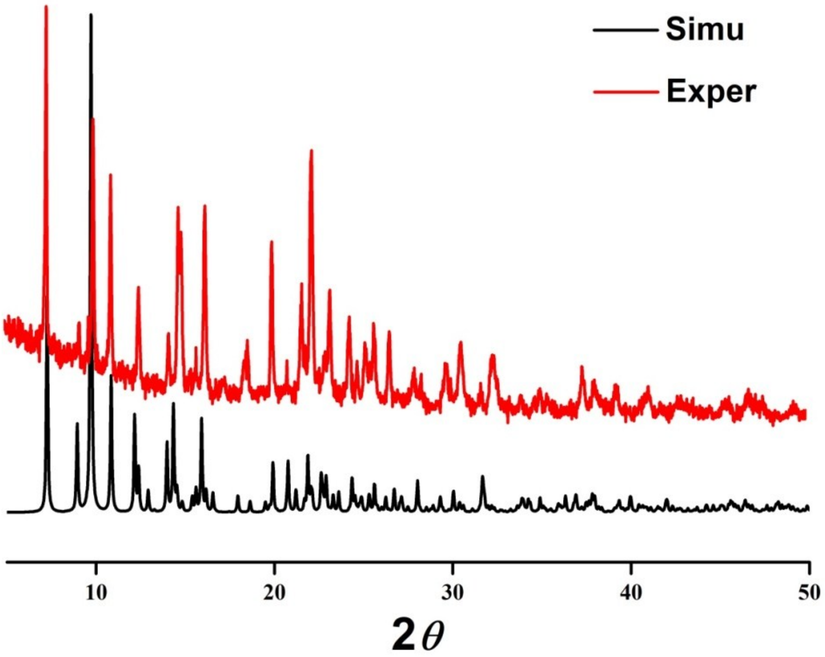

Fig. **S1** PXRD patterns of **Cd-MOF** simulated from the X-ray single-crystal data and as-synthesized products.

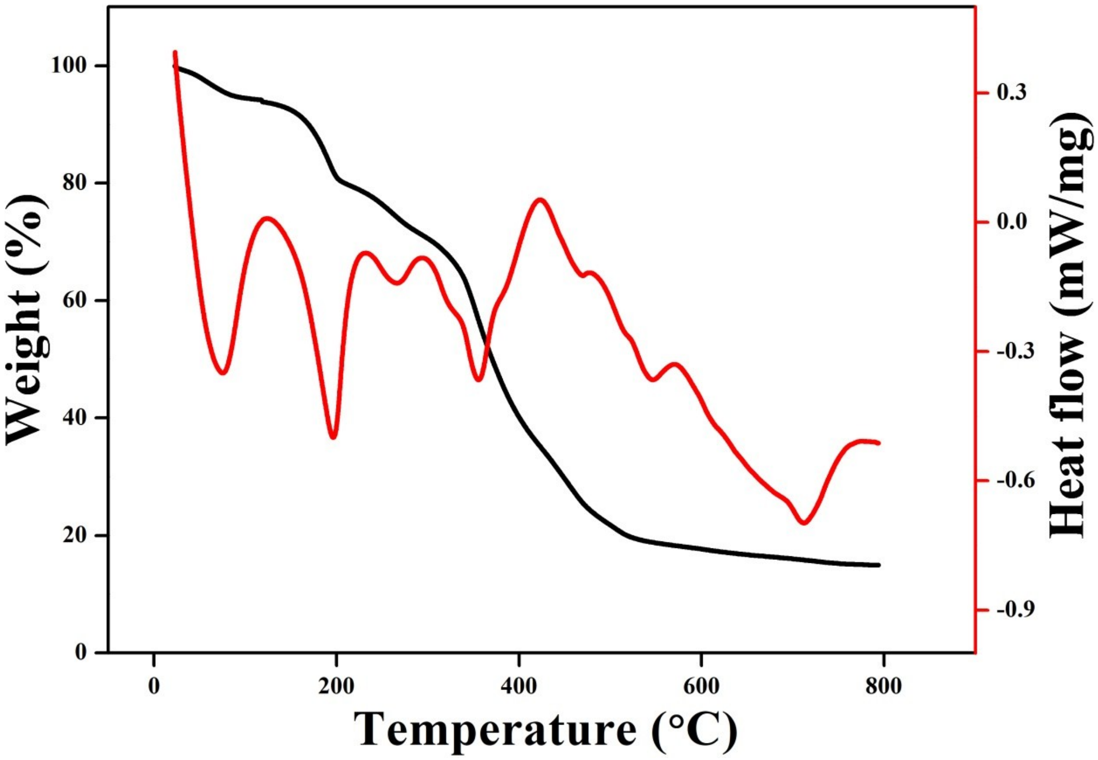

Fig. **S2** TG and DSC curves for **Cd-MOF**.

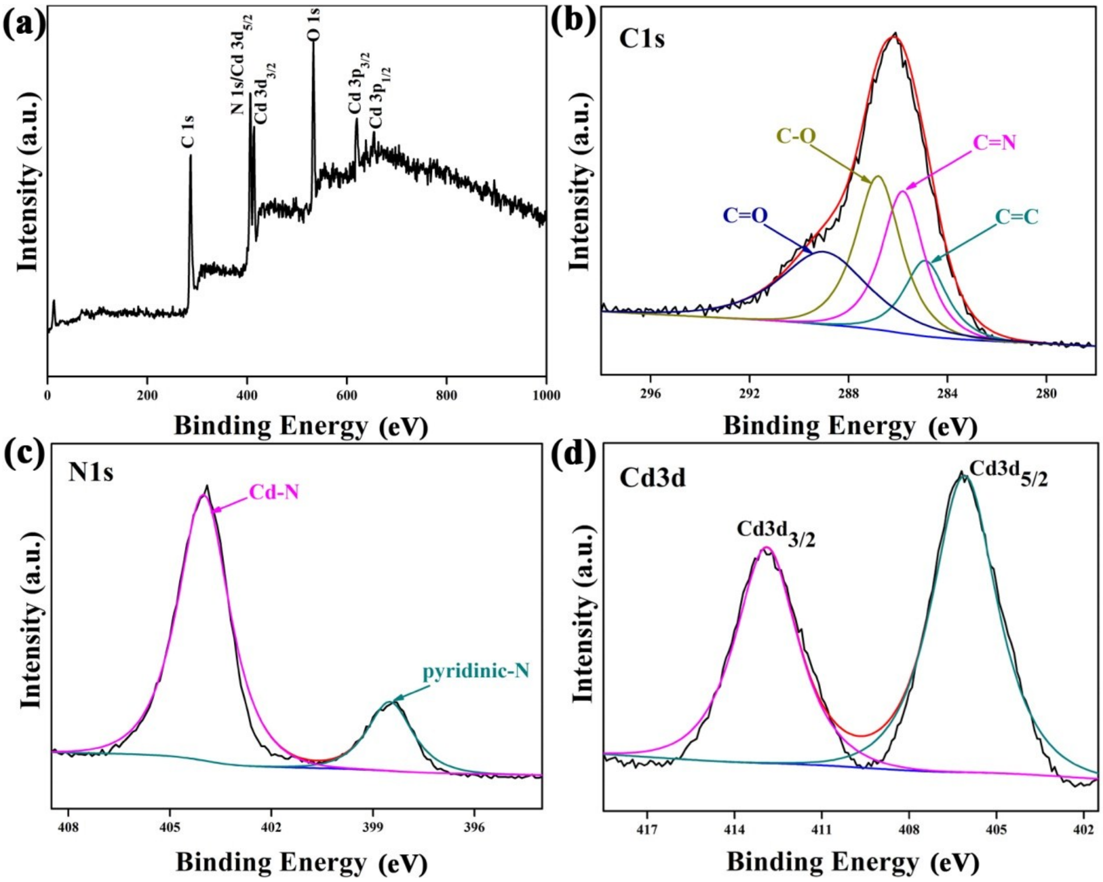

Fig. **S3** XPS spectra of **Cd-MOF**: (**a**) survey; (**b**) C 1s; (**c**) N 1s and (**d**) Cd 3d

Fig. **S3b** shows the high-resolution XPS spectrum of C 1s, which can be deconvoluted into four peaks on the basis of their binding energies, corresponding to C=C (284.9 eV), C=N (285.8 eV), C-O (286.8 eV) and C=O (289 eV). In the high-resolution spectrum of Fig. **S3c**, the N 1s spectrum can be separated into two main peaks. The binding energy at 398.5 eV is attributed to pyridinic-N, whereas the binding energies of 404 eV are assigned to the interaction between Cd and N. The XPS spectrum of O 1s displayed in Fig. **5a** shows the peaks at 530.5 eV, 531.3 eV, 532.2 eV, 533 eV and 533.9 eV, indicating the existence of Cd-O bonds, hydroxyl oxygen, carbon-oxygen double bond, carbon-oxygen single bond and physi- or chemi-sorbed water/oxygen, respectively. It is observed from Fig. **S3d**, the two peaks at the binding energy levels of 406.1 eV and 412.9 eV, corresponding to Cd $3d_{5/2}$ and Cd $3d_{3/2}$, respectively. There is spin orbit separation of about 6.8 eV between Cd $3d_{5/2}$ and Cd $3d_{3/2}$ states, which agrees well with previous reported.

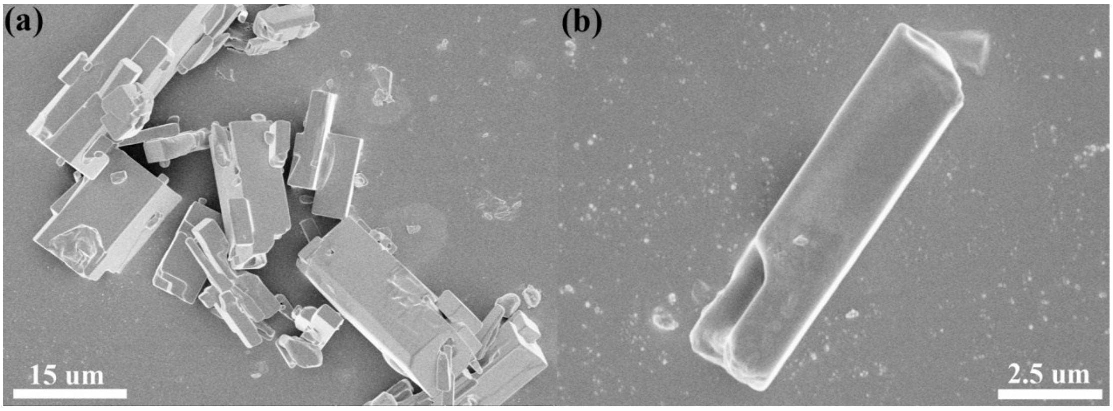

Fig. **S4** SEM images of **Cd-MOF**.

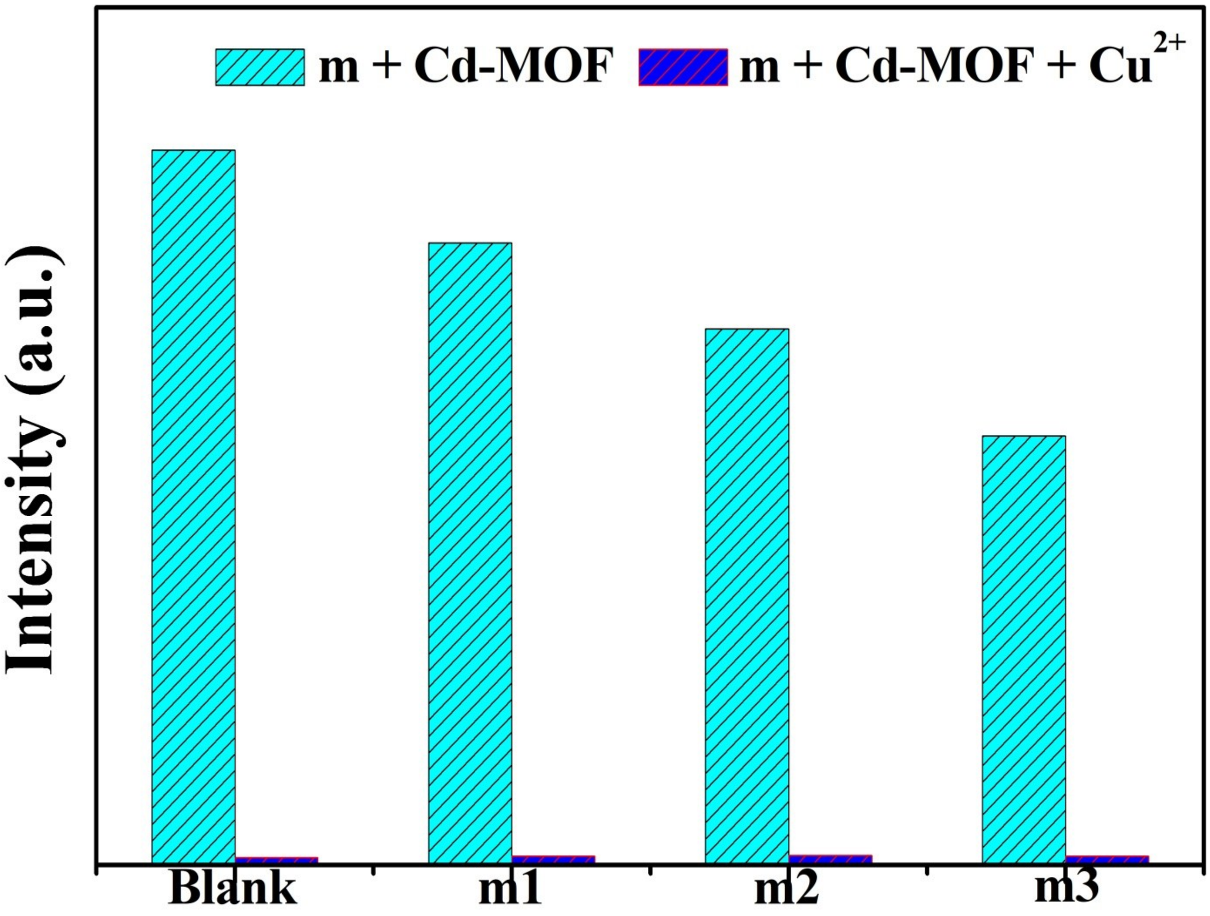

Fig. **S5** Luminescence intensity of **Cd-MOF** at 461 nm dispersed in water with the addition of different mixed ions (0.01 M) (m1: Cd^{2+}/Pb^{2+}; m2: $Ca^{2+}/Zn^{2+}/Ni^{2+}$; m3: Co^{2+} /Hg^{2+}/Mn^{2+} /Ni^{2+}).

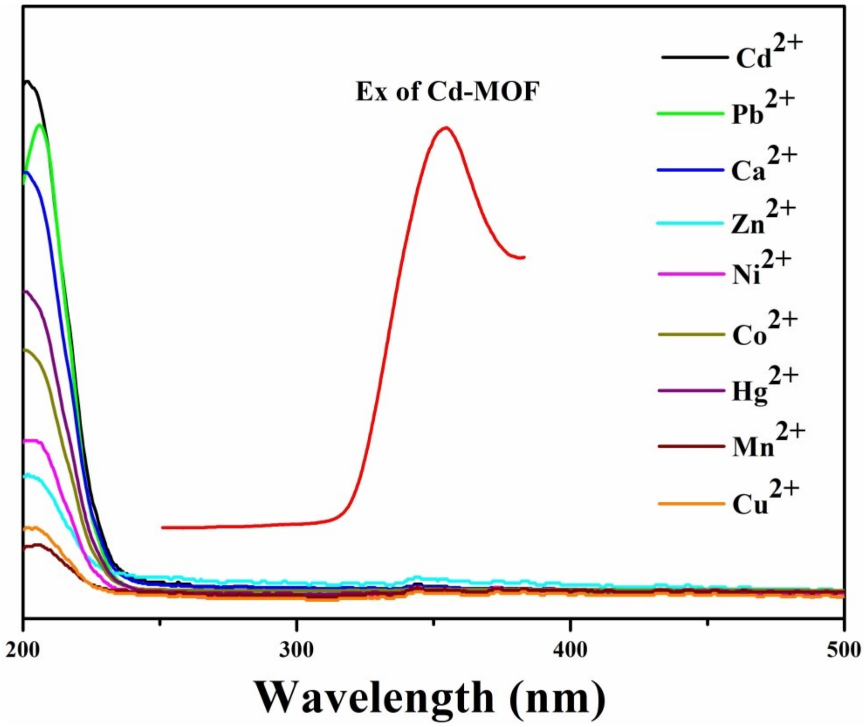

Fig. **S6** UV-vis adsorption spectra of M $(NO_3)_n$ aqueous solutions and the excitation spectrum of **Cd-MOF**.

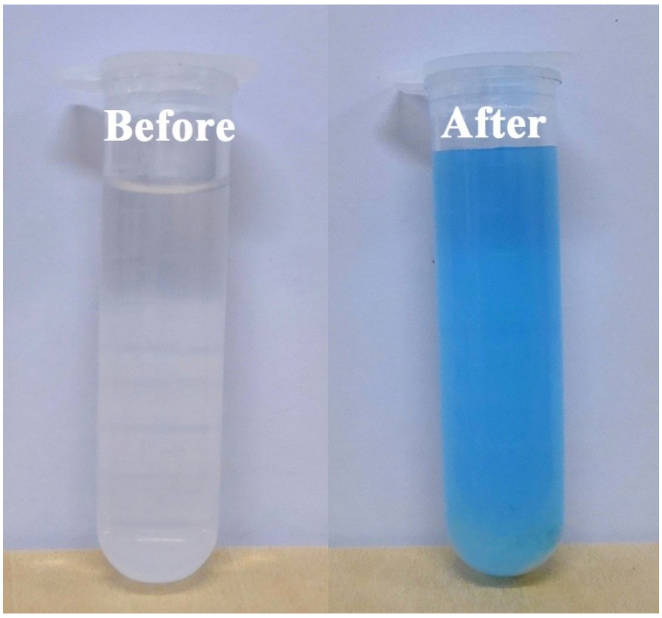

Fig. **S7** The color images before and after adding **Cd-MOF** into $Cu(NO_3)_2$ aqueous solutions.

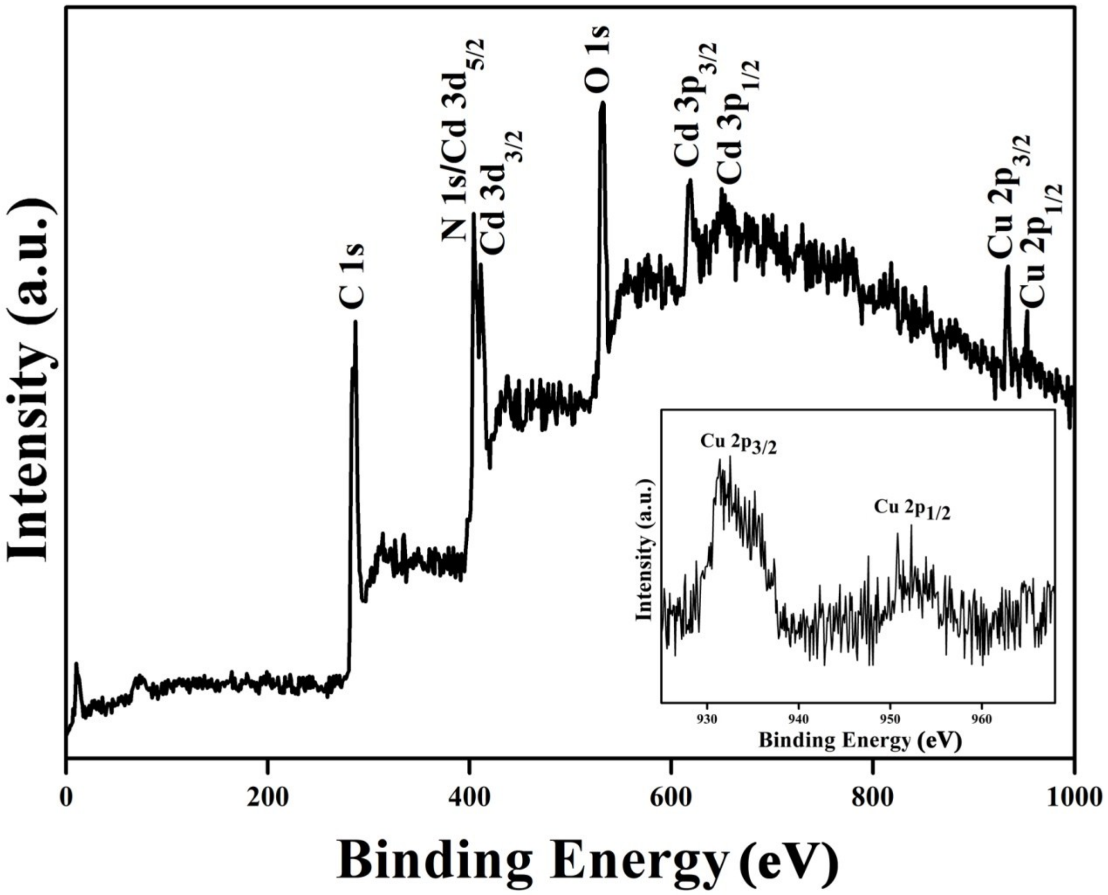

Fig. **S8** XPS survey for Cu^{2+} treatment of **Cd-MOF**.

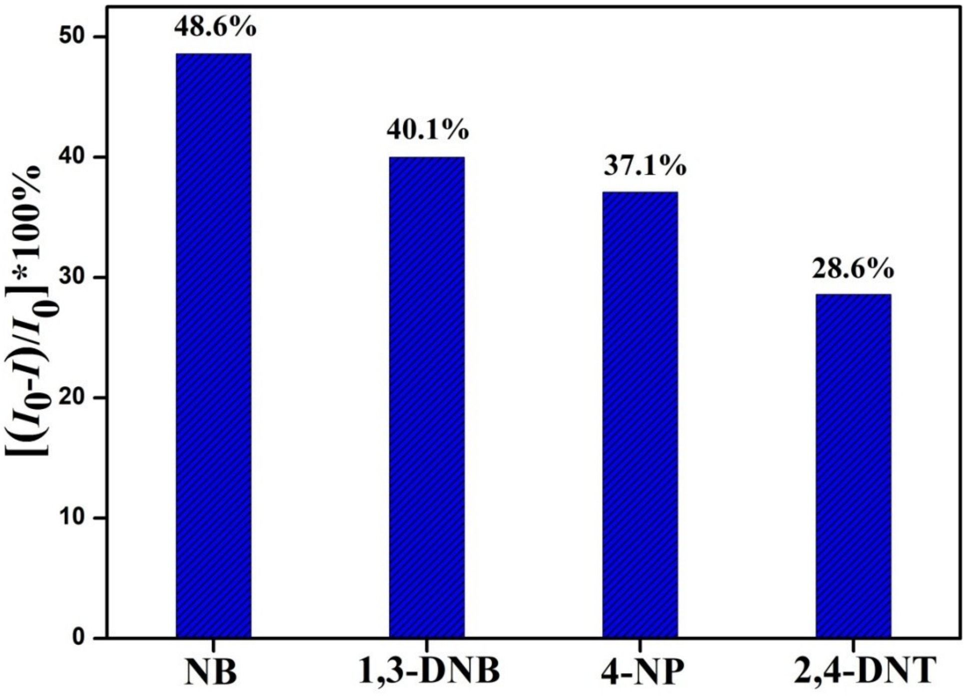

Fig. **S9** The luminescence quenching efficiencies of nitro-compounds with the same concentration (0.1 mM).

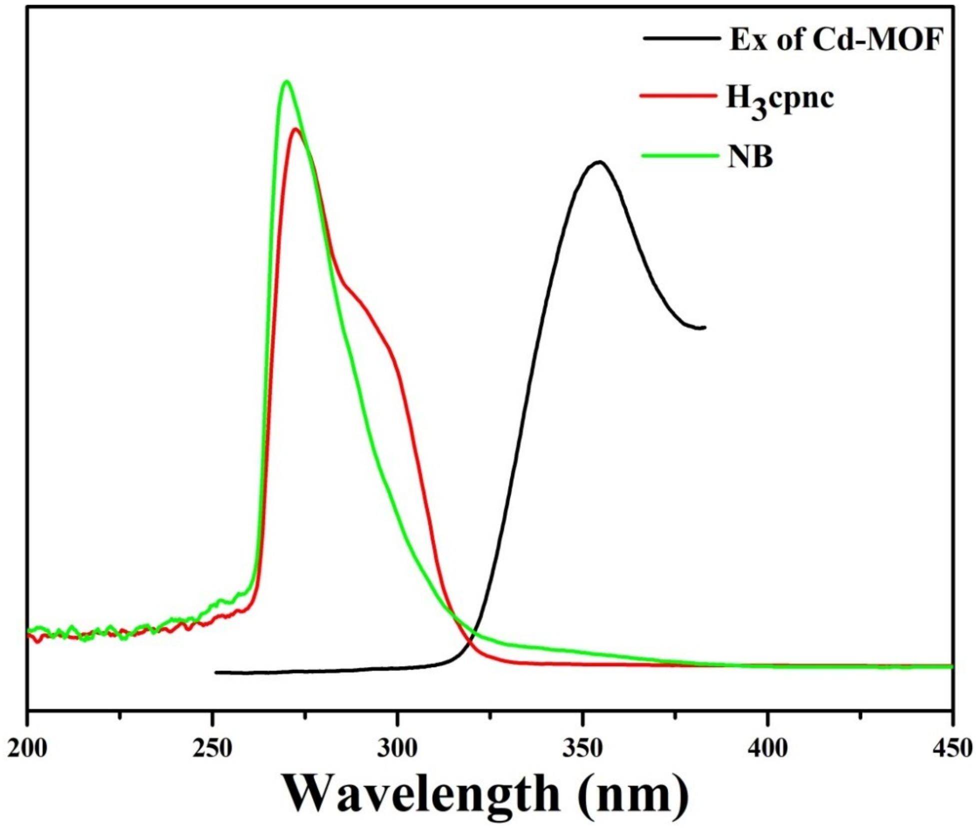

Fig. **S10** UV-vis adsorption spectra of NB and H_3cpnc in DMA solution, and the excitation spectrum of **Cd-MOF**.

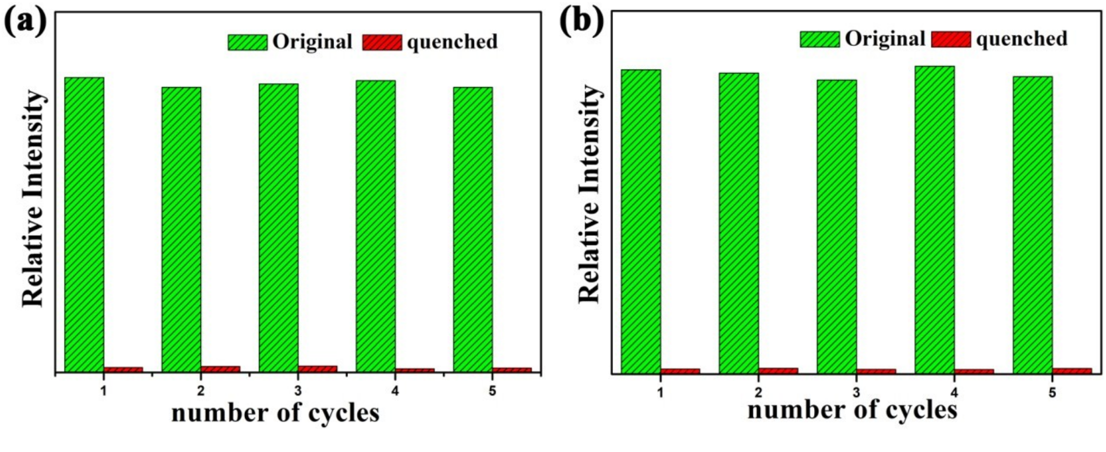

Fig. **S11** Luminescent intensity at 461 nm of **Cd-MOF** after five recycles in (a) Cu^{2+} and (b) NB solutions (10^{-2} M)

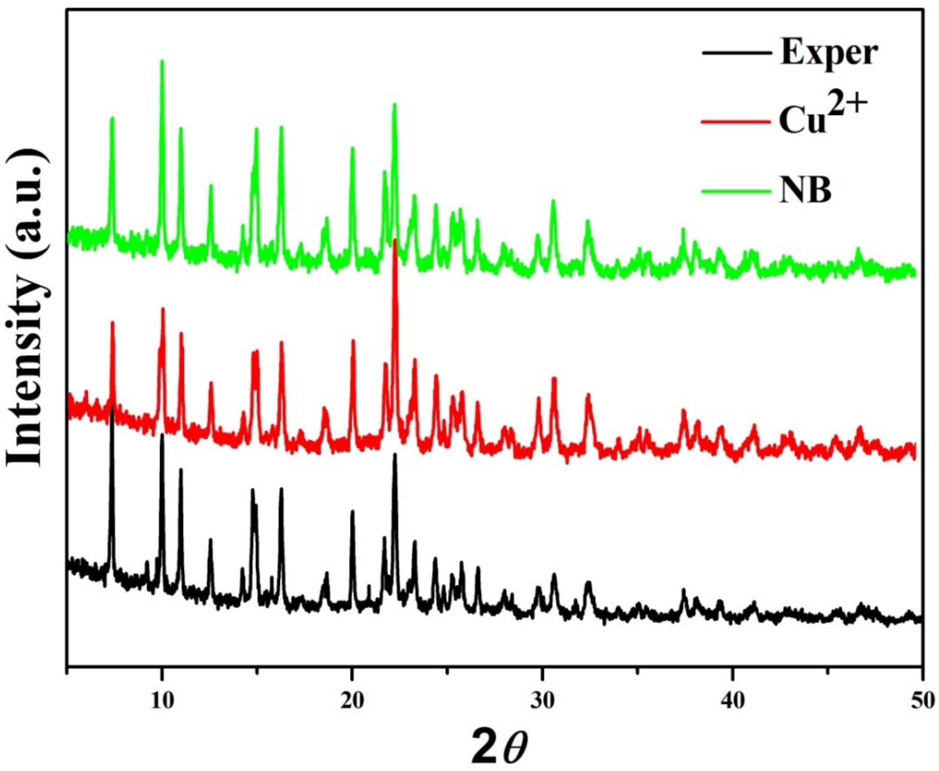

Fig. **S12** PXRD patterns of **Cd-MOF** treated by the Cu^{2+} ion aqueous solution and NB after five runs

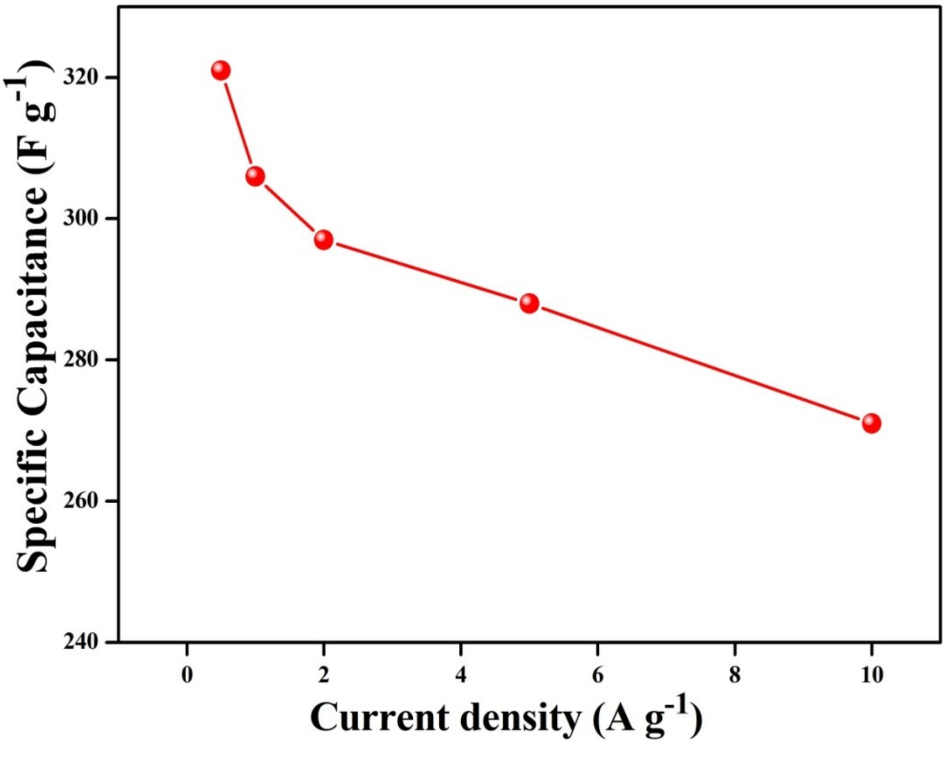

Fig. **S13** The gravimetric capacitance for **Cd-MOF** electrode at various current densities.

Table S1 Comparison of supercapacitive performance of our sample with other previously reported MOF-based electrode materials.

MOF-based materials	**Specific capacitance**	**Current density /Scan rate**	**Retention (%)**	**Electrolyte**	**Reference**
Cu@BTC	228 F g^{-1}	1.5 A g^{-1}	89	3 M KOH	35
$[Ni(Hppza)_2]_n$	184 F g^{-1}	5 mV s^{-1}	65	2 M KOH	36
Co-MOF	206.8 F g^{-1}	0.6 A g^{-1}	98	0.5 M LiOH	37
Ni-pPD	295 F g^{-1}	2 A g^{-1}	80	$TEABF_4$/ACN	38
Cu-bipy-BTC	160 F g^{-1}	0.005 mA g^{-1}	93	0.1 M $HClO_4$	39
Co-BPDC	179.2 F g^{-1}	10 mV s^{-1}	77	0.5 M LiOH	40
Cd-MOF	321 F g^{-1}	0.5 A g^{-1}	95.2	2 M KOH	**This Work**